Journal of Power Sources 195 (2010) 6122–6129

Contents lists available at ScienceDirect

Journal of Power Sources

journal homepage: www.elsevier.com/locate/jpowsour

Surface modification of $Li[Ni_{0.3}Co_{0.4}Mn_{0.3}]O_2$ cathode by Li–La–Ti–O coating

Hye Jin Lee [a], Kyu-Sung Park [b], Yong Joon Park [a,*]

[a] Department of Advanced Materials Engineering, Kyonggi University, San94-6, Yiui-dong, Yeongtong-gu, Gyeonggi-do 443-760, Republic of Korea
[b] Battery Group, Samsung Advanced Institute of Technology (SAIT), Yongin 446-712, Republic of Korea

ARTICLE INFO

Article history:
Received 30 September 2009
Accepted 29 October 2009
Available online 5 November 2009

Keywords:
Cathode
Surface coating
Lithium battery
Solid electrolyte

ABSTRACT

A $Li[Ni_{0.3}Co_{0.4}Mn_{0.3}]O_2$ cathode is modified by applying a Li–La–Ti–O coating using the hydrothermal method. The coated $Li[Ni_{0.3}Co_{0.4}Mn_{0.3}]O_2$ is characterized by X-ray diffraction analysis, scanning electron microscopy, energy-dispersive spectrometry, transmission electron microscopy, and differential scanning calorimetry. The Li–La–Ti–O coating layer is formed as crystalline (perovskite structure) or amorphous phase depending on the heating temperature. The Li–La–Ti–O coated $Li[Ni_{0.3}Co_{0.4}Mn_{0.3}]O_2$ electrode has better rate capability than the pristine electrode. In particular, the rate capability is significantly associated with heating temperature; this is probably due to the phase of the coating layer. It appears that the Li–La–Ti–O coating of amorphous phase is superior to that of crystalline phase for obtaining enhanced rate capability of the coated samples. The thermal stability and cyclic performance of the $Li[Ni_{0.3}Co_{0.4}Mn_{0.3}]O_2$ electrode are also improved by Li–La–Ti–O coating. These improvements indicate that the Li–La–Ti–O coating is effective in suppressing the chemical and structural instabilities of $Li[Ni_{0.3}Co_{0.4}Mn_{0.3}]O_2$.

1. Introduction

Since Sony announced the commercial availability of rechargeable lithium batteries, they have been widely used as power sources for cellular phones, PDAs, and notebook computers. Nowadays, the lithium battery industry has branched out new applications such as electric vehicles (EVs), hybrid electric vehicles (HEVs), plug-in hybrid electric vehicles (PHEVs) and electric power tools [1–4]. These new products are expected to open a huge lithium battery market and lead to the setting up of related industries. In order to meet the challenging requirements of these new applications, the cathode material, a core constituent of lithium batteries, needs to be significantly improved in terms of cost, safety, power, energy density, and cycle life. One approach to improve these properties is coating treatment of the surface of cathode powder with stable coating materials. There have been several reports that physical and chemical properties are significantly improved by coating with oxides [5–11], phosphates [12–17], and fluorides [18,19]. Coatings result in reduced cation dissolution during cycling, lower impedance resistance of the interface between cathode and electrolyte, and enhanced structural stability at high voltage. One of the most interesting results is the fact that the rate capability can be enhanced by surface coating. Basically, the coating materials are non-conductive materials of lithium ions and electrons, so they may act as an obstacle to the diffusion of lithium ions and electrons. However, the surface coating suppresses the formation of an unwanted surface layer originating from the dissolution of cations (e.g., Co, Ni, and Mn...) and/or the attack of HF in the electrolyte [11–14]. The unwanted surface layer is a major obstacle to lithium and electron diffusion, so suppression of the unwanted layer facilitates the movement of lithium ions and electrons. However, it is possible that the surface coating layer itself is a hindrance to the diffusion of lithium ions and electrons.

Herein, we introduce a solid electrolyte (Li–La–Ti–O type) as a coating material to enhance the conductivity of the coating layer and increase the rate capability. Li–La–Ti–O is a good solid electrolyte owing to its high ion conductivity of $\sim 10^{-3}$ Scm^{-1} at room temperature [20–25]. Moreover, it has higher electronic conductivity than other solid electrolytes. The high electronic conductivity is a major problem in using Li–La–Ti–O as a solid electrolyte, but it is a great advantage for a coating material. It is expected that a positive electrode coated with Li–La–Ti–O will have a greater rate capability owing to the coating with high ionic and electronic conductivity, as well as good cyclic performances and thermal stability owing to the protection effect from reactive electrolyte.

Commercial $Li[Ni_{0.3}Co_{0.4}Mn_{0.3}]O_2$, which is a promising cathode material owing to its high discharge capacity and stable cycle life, was used as a pristine powder. The hydrothermal method for coating was adopted to achieve a more uniform coating. Generally, coating is applied by mixing cathode powders and coating solution followed by drying and heat-treatment (i.e., a typical wet

* Corresponding author. Tel.: +82 31 249 9769; fax: +82 31 249 9769.
E-mail addresses: yjpark2006@kyonggi.ac.kr, yjparketri@yahoo.co.kr (Y.J. Park).

0378-7753/$ – see front matter © 2009 Elsevier B.V. All rights reserved.
doi:10.1016/j.jpowsour.2009.10.080

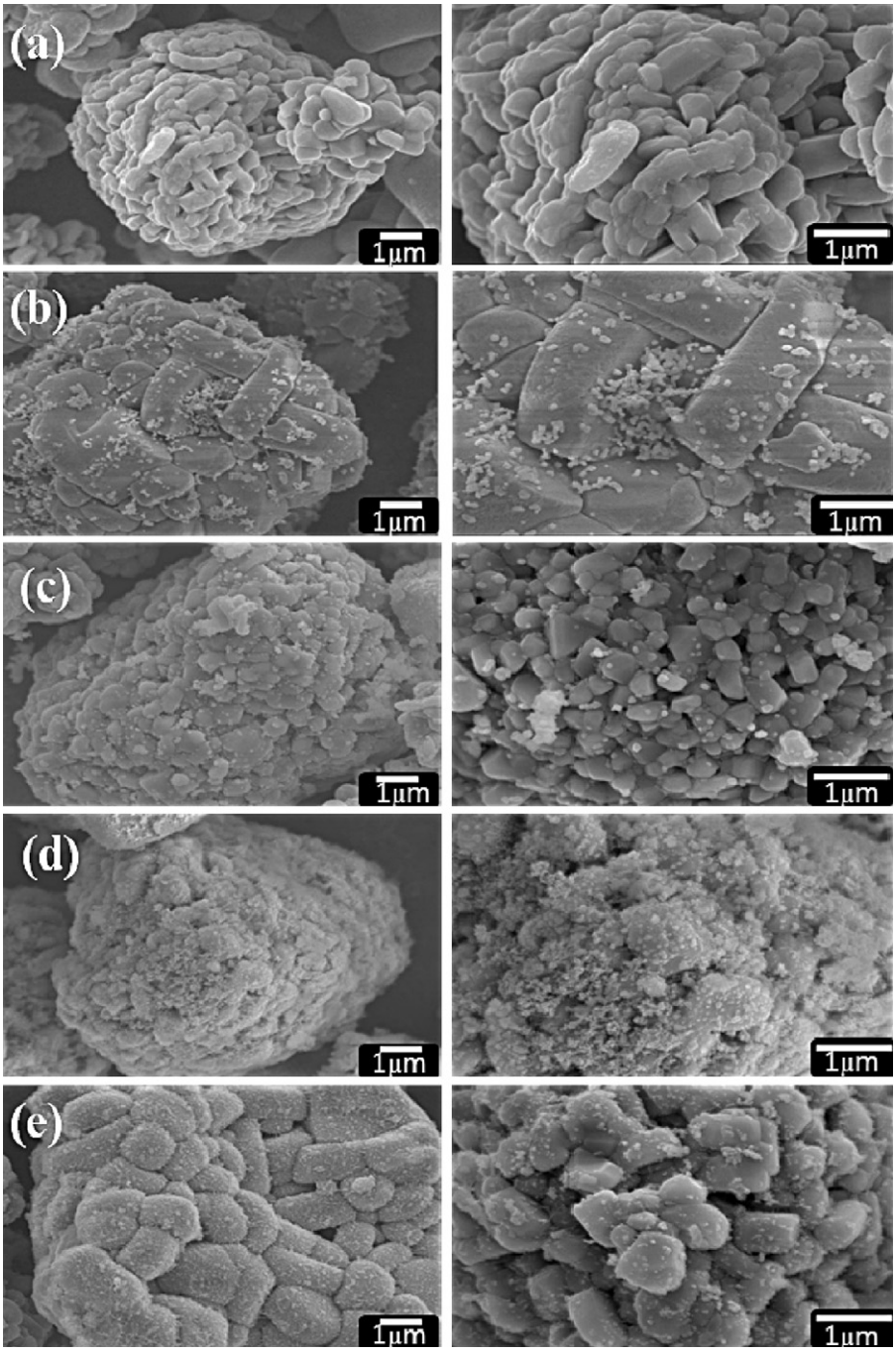

Fig. 1. SEM images of $Li[Ni_{0.3}Co_{0.4}Mn_{0.3}]O_2$ powder. (a) Pristine; (b) 700A; (c) 700B; (d) 400A; (e) 400B.

process). However, the hydrothermal method employing temperature and pressure to react the cathode and coating solution, can achieve a more uniform coating on the surface of a pristine cathode. In this study, Li–La–Ti–O was coated on the surface of a $Li[Ni_{0.3}Co_{0.4}Mn_{0.3}]O_2$ cathode using the hydrothermal method and the electrochemical and structural properties of the coated electrode were examined. Thermal stability was also investigated to determine the coating effect.

Table 1
Discharge capacities and capacity retentions of pristine and coated $Li[Ni_{0.3}Co_{0.4}Mn_{0.3}]O_2$ samples at various C rates (values of the initial cycle at respective C rates). (The percentages refer to capacity retention compared with the discharge capacity at the 0.5 C rate).

	Pristine (mAh g^{-1})	(%)	700A (mAh g^{-1})	(%)	700B (mAh g^{-1})	(%)	400A (mAh g^{-1})	(%)	400B (mAh g^{-1})	(%)
0.5 C	179.25	100.0	175.8	100.0	175.23	100.0	173.9	100.0	177.02	100.0
1 C	157.71	88.0	159.19	90.6	158.44	90.4	158.70	91.3	160.15	90.5
2 C	128.81	71.9	143.71	81.8	144.07	82.2	143.25	82.4	143.19	80.9
3 C	105.73	59.0	129.72	73.8	123.32	70.4	131.27	75.5	130.26	73.6
6 C	55.72	31.1	92.06	52.4	89.55	51.1	103.74	59.7	99.62	56.3

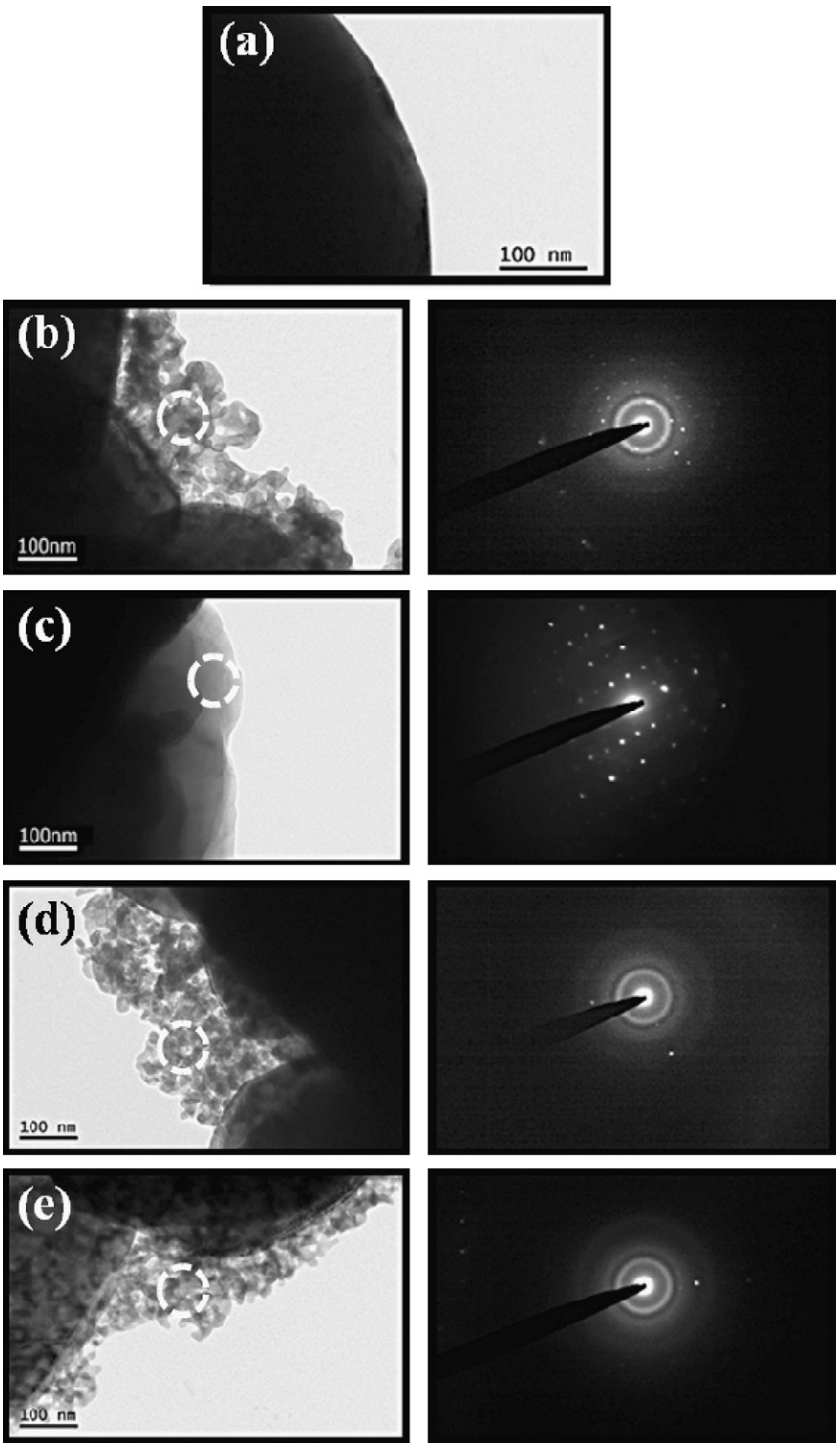

Fig. 2. TEM images of $Li[Ni_{0.3}Co_{0.4}Mn_{0.3}]O_2$ powder. (a) Pristine; (b) 700A; (c) 700B; (d) 400A; (e) 400B. The images on the right are spot patterns of the area marked in the white circle in the TEM images.

2. Experimental

Pristine $Li[Ni_{0.3}Co_{0.4}Mn_{0.3}]O_2$ powder was supplied by Daejung Chemicals & Metals. To prepare Li–La–Ti–O coating solution, lithium nitrate [$LiNO_3$] (Aldrich), lanthanum(III) nitrate hexahydrate [$La(NO_3)_3{\cdot}6H_2O$] (99.99%, Aldrich), and titanium(IV) isopropoxide [$Ti(OCH(CH_3)_2)_4$] (97%, Aldrich) were dissolved in isopropanol and ammonium solution was added while the mixture was continuously stirred at 50–60 °C on a hot plate. The molar ratio of Li:La:Ti sources was 0.5:0.5:1. (Coating material was assumed as $Li_{0.5}La_{0.5}TiO_3$). The solution was clear before the addition of ammonium, but as more ammonium was added, the solution turned into a colloid-type solution. We tested two types of solution for the coating treatment, one was a clear coating solution, for which 0.2 g of 3 wt.% ammonium solution was added to 12 g of source solution (containing 0.002 mol organic sources), and the other was a colloid-type coating solution, for which 0.4 g of 3 wt.% ammonium solution was added to 12 g of source solution. Pristine $Li[Ni_{0.3}Co_{0.4}Mn_{0.3}]O_2$ powder was added to the coating solution and well mixed. The mixture was introduced into a Parr bomb and heated to 120 °C for 15 h

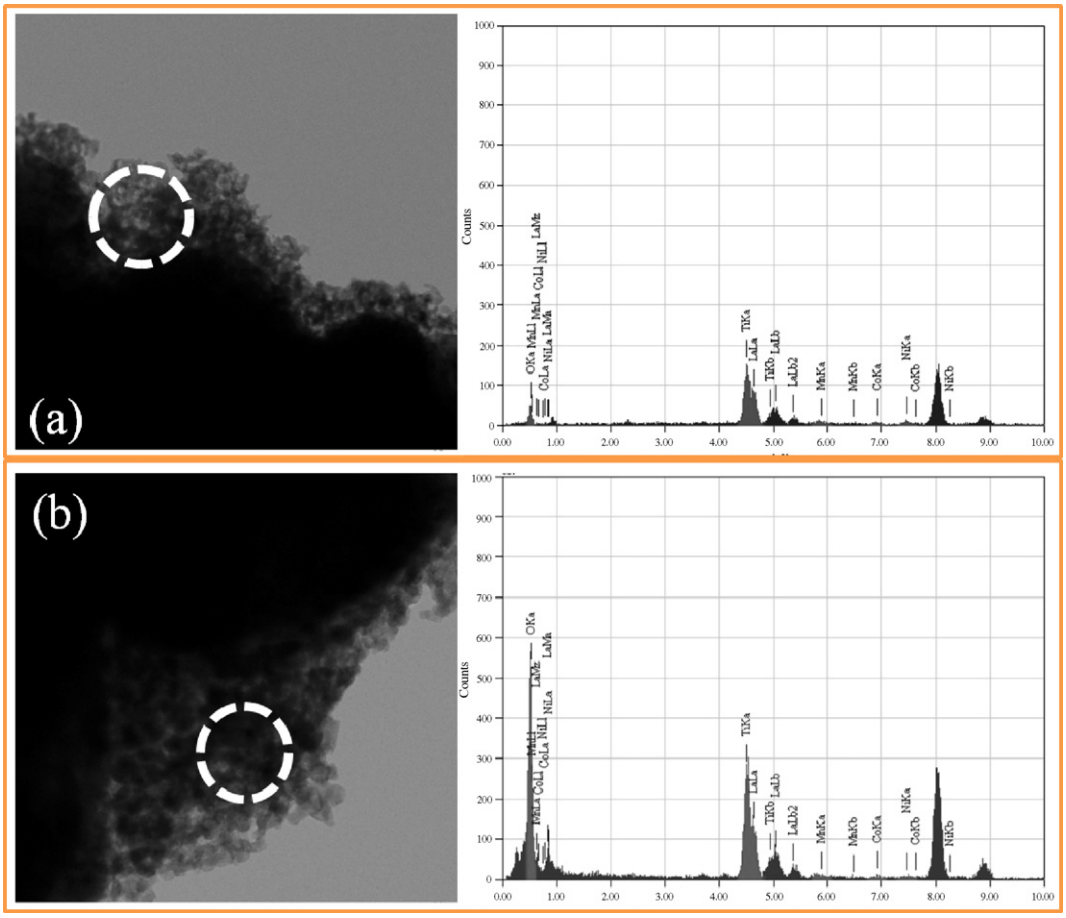

Fig. 3. EDS peaks of coated $Li[Ni_{0.3}Co_{0.4}Mn_{0.3}]O_2$ powder. (a) 700A; (b) 400A.

to produce a hydrothermal reaction. Afterward, the slurry was dried and heat-treated in a furnace at 400 and 700 °C for 6 h to obtain Li–La–Ti–O coated $Li[Ni_{0.3}Co_{0.4}Mn_{0.3}]O_2$ powder. X-ray diffraction (XRD) patterns of powders were obtained using a Rigaku X-ray diffractometer in the 2θ range of 10–70° with monochromatized Cu-K_α radiation (λ = 1.5406 Å). The microstructure of the powder was observed by field-emission scanning electron microscopy (FE-SEM, JEOL-JSM 6500F). Transmission electron microscopy (FE-TEM, JEOL-JEM 2100F) was also carried out with an electron microscope, operating at 200 kV.

The cathodes for electrochemical studies were prepared using a doctor-blade coating method with a slurry of 80 wt.% coated active material, 12 wt.% conductive carbon(Super-P) and 8 wt.% poly vinylidene fluoride (PVDF) in N-methyl-2-pyrrolidone (NMP), as the solvent for the mixture. It was then applied to an aluminum foil current collector and dried at 90 °C in an oven. The coated cathode foil was cut into circular discs 12 mm in diameter. The electrochemical performances of the discs were evaluated with coin-type cells of the 2032 configuration and the discs were assembled in an argon-filled glove box. Lithium metal was used as the anode. The electrolyte was 1 M $LiPF_6$ with ethylene carbonate/dimethyl carbonate (EC/DMC) (1:1, vol.%). Cells were subjected to galvanostatic cycling using a WonAtech system in the voltage range of 4.6–3.0 V at rates of 1–6 C.

Differential scanning calorimetry (DSC) samples for the cathode were prepared by the following treatment before testing. Cells containing sample electrodes were charged to 4.6 V with a current density of 36 mAg^{-1}, and the potential was held until the current density reached 4 mAg^{-1}. The cells were then disassembled in a dry room to remove the charged positive electrode. 5 mg of the positive electrode including electrolyte was sealed in a high-pressure DSC pan. The heating rate and temperature range in the DSC tests were 5 °C min^{-1} and 25–350 °C, respectively.

3. Results and discussion

$Li[Ni_{0.3}Co_{0.4}Mn_{0.3}]O_2$ was coated with the two types of coating solution. The coated samples were named 700A (coated with colloid-type solution and heat-treated at 700 °C), 700B (coated with clear solution and heat-treated at 700 °C), 400A (coated with colloid-type solution and heat-treated at 400 °C), and 400B (coated with clear solution and heat-treated at 400 °C). Fig. 1 presents scanning electron microscopy (SEM) images of pristine and Li–La–Ti–O coated samples. The pristine powder appears as 5–8 μm spheres composed of smooth-edged 0.2–0.5 μm polyhedral primary particles. The crystal faces and edges on the surface of the pristine $Li[Ni_{0.3}Co_{0.4}Mn_{0.3}]O_2$ are very clear. In comparison, the surfaces of the coated samples were covered by fine nano-particles 10–50 nm in size. It seems that the coating particles of 700B and 400B were more uniformly distributed than those of 700A and 400A, which indicates the clear coating solution is better than the colloid-type coating solution in forming a uniform coating layer. The surfaces of the powders were not perfectly encapsulated by the coating layers. However, coating particles easily migrated into the lattice of the parent powder during heating treatment and cycling because the surface free energy of these nano-particles is very high owing to their size [26]. Thus, portions of the surfaces of coated powders, those are not directly in con-

Table 2
Discharge capacities (1st and 50th cycles) and capacity retentions (during 50 cycles) of $Li[Ni_{0.3}Co_{0.4}Mn_{0.3}]O_2$ samples in the voltage range of 4.8-3.0 V at the 1 C rate.

	Pristine (mAh g^{-1})	(%)	700A (mAh g^{-1})	(%)	700B (mAh g^{-1})	(%)	400A (mAh g^{-1})	(%)	400B (mAh g^{-1})	(%)
1st	187.92	68.6	193.45	72.5	193.11	71.2	193.54	69.1	187.24	74.3
50th	128.84		140.17		137.54		133.68		139.06	

tact with coating particles, may also be affected by the coating elements.

Transition electron microscopy (TEM) images of the pristine and Li–La–Ti–O coated samples are shown in Fig. 2. The right TEM images show spot patterns of the coating layers. The coating layers of 700A and 700B samples, which were heat-treated at 700 °C, were crystalline or quasi-crystalline containing amorphous phase a little. In particular, the spot pattern of the coating layer of 700B was clear, indicating good crystallinity. In contrast, the coating layers of 400A and 400B, which were heat-treated at 400 °C, seem to have an amorphous phase. This difference may be attributed to the heating temperature after coating treatment. Generally, Li–La–Ti–O solid electrolyte with high ionic conductivity is a crystalline phase (perovskite). However, most solid electrolytes are amorphous phases because the flexible structure of an amorphous phase can facilitate the diffusion of ions. The phase of the coating layer may be associated with electrochemical properties such as the rate capability. The elements of the coating layer were confirmed by TEM-EDS analysis, as shown in Fig. 3. The detection of clear peaks corresponding to La and Ti confirm that the Li–La–Ti–O coating layer successfully formed on the surface of pristine $Li[Ni_{0.3}Co_{0.4}Mn_{0.3}]O_2$ powder.

Fig. 4 shows XRD patterns of the pristine and Li–La–Ti–O coated $Li[Ni_{0.3}Co_{0.4}Mn_{0.3}]O_2$ powders. All the observed peaks for pristine powder can be indexed to a hexagonal α-$NaFeO_2$ structure (space group: R-3m). The diffraction patterns of 400A and 400B powders

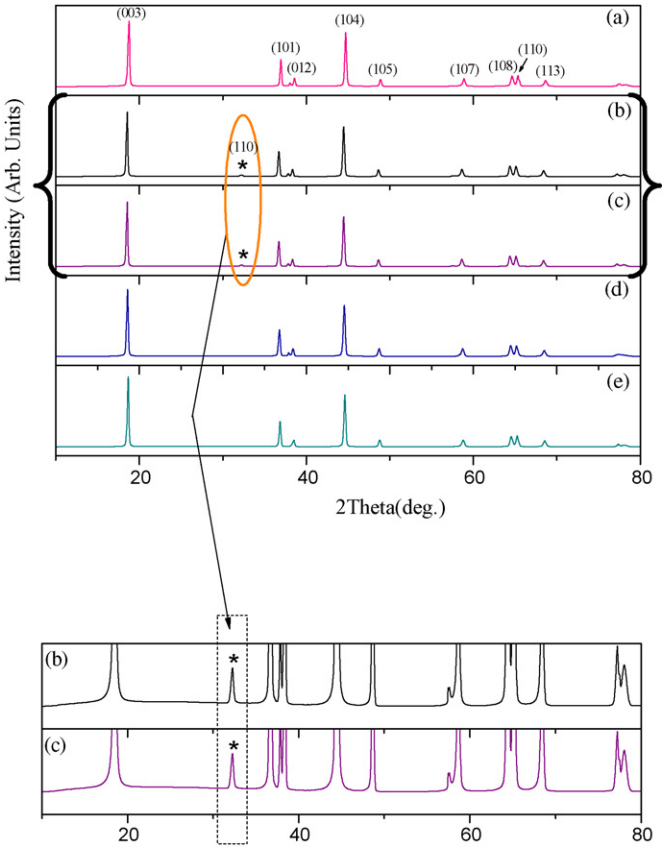

Fig. 4. XRD patterns of $Li[Ni_{0.3}Co_{0.4}Mn_{0.3}]O_2$ samples. (a) Pristine; (b) 700A; (c) 700B; (d) 400A; (e) 400B.

are identical to those of the pristine sample, even though a coating layer has formed on the surface. This also indicates that the coating layer of the samples heat-treated at 400 °C is an amorphous phase. However, the crystalline phase of the coating layer was clearly detected in the diffraction patterns of 700A and 700B. The small peak at $2\theta = 32.2^{o}$ corresponds to the (1 1 0) reflection of the typical Li–La–Ti–O perovskite structure, which indicates that the coating layer of samples heat-treated at 700 °C is a crystalline phase with perovskite structure. This is consistent with the result of TEM analysis in Fig. 2. Apart from a small peak associated with the coating material, a structural change in the pristine powder due to surface coating and heat-treatment was not observed in the XRD patterns.

The electrochemical properties of the pristine and coated $Li[Ni_{0.3}Co_{0.4}Mn_{0.3}]O_2$ electrodes were characterized to examine the coating effect on capacity, cyclic performance, and rate capability. Fig. 5 shows the discharge capacity and cyclic property of the pristine and coated $Li[Ni_{0.3}Co_{0.4}Mn_{0.3}]O_2$ electrodes at different C rates. The cells were cycled at 0.5, 1–3, and 6C rates in the voltage range of 4.6–3.0 V at a constant temperature of 30 °C. All samples had a similar discharge capacity for several initial cycles at rates of 0.5 and 1 C. However, the Li–La–Ti–O coated samples had obviously higher capacity at rates of 2, 3 and 6 C. It is clear that the Li–La–Ti–O coating was effective in achieving higher rate capability with respect to the delivered capacity. Table 1 summarizes the discharge capacity and capacity retention at various C rates (the values of initial cycles at respective C rates). From the table, it is apparent that the ratio of the discharge capacity at a high C rate to that at a 0.5 C rate was increased by the coating treatment. The capacity retention for the pristine electrode at the 6 C rate was only ~31%, compared with that at 0.5 C rate. However, coated samples had more than 50% capacity retention under the same measurement condition. Fig. 6 shows the voltage profiles of pristine and Li–La–Ti–O coated samples at 3 and 6 C rates as functions of the capacity. The coated samples had higher discharge capacity at both C rates. The ability of a surface coating to enhance the rate capabil-

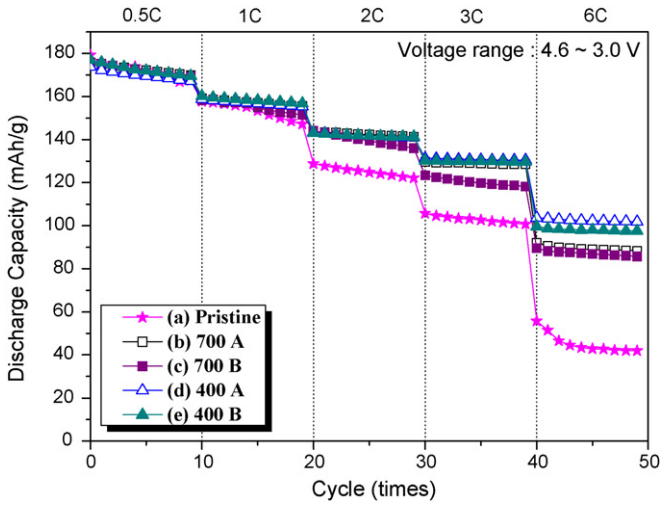

Fig. 5. Discharge capacities and cyclic performances of pristine and coated $Li[Ni_{0.3}Co_{0.4}Mn_{0.3}]O_2$ electrodes in the voltage range of 4.6–3.0 V at 0.5, 1, 2, 3, and 6 C rates.

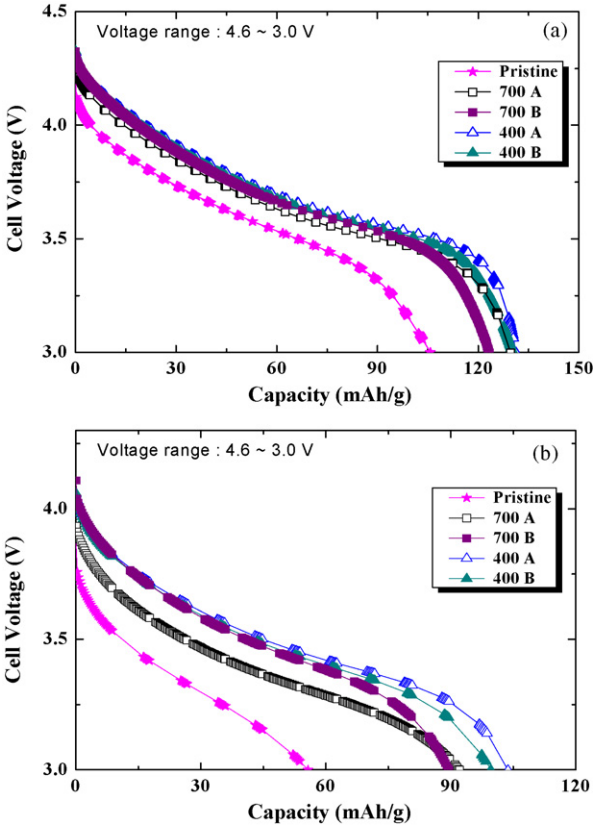

Fig. 6. Initial discharge profiles of pristine and Li–La–Ti–O coated $Li[Ni_{0.3}Co_{0.4}Mn_{0.3}]O_2$ electrodes in the voltage range of 4.6–3.0 V at (a) 3 C and (b) 6 C rates.

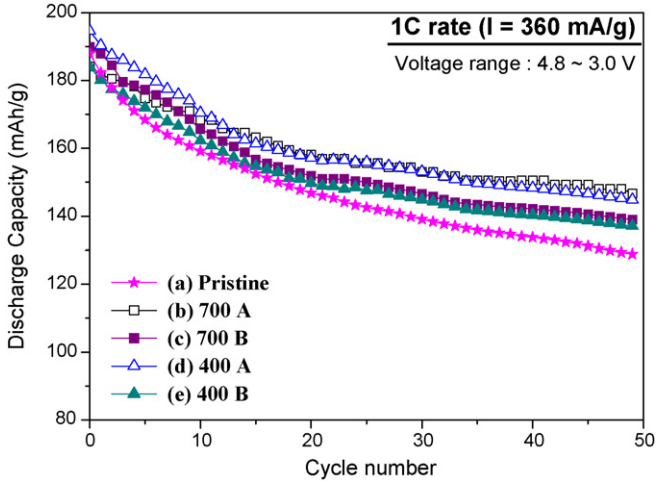

Fig. 7. Cyclic performance of $Li[Ni_{0.3}Co_{0.4}Mn_{0.3}]O_2$ electrodes in the voltage range of 4.8–3.0 V at the 1 C rate.

ity has been previously reported [12–19]. $LiPF_6$ salt in electrolyte produces HF via reaction with moisture in the air. The HF attacks the surface of the cathode, and thus the cations (Co, Ni, and Mn ions) in the structure of the cathode dissolve into the electrolyte, and an interface layer, which interrupts the diffusion of lithium ions and electrons, forms on the surface of the cathode [11]. However, the coating material can act as a HF scavenger and reduce the unwanted reaction between the electrode and electrolyte. The enhanced rate capability of the coated samples may be attributed to the reduction of cation dissolution and suppression of the formation of a surface interface layer. Moreover, the high ionic conductivity of the coating material (Li–La–Ti–O) may increase the rate capability. It is interesting that the samples heat-treated at 400 °C (400A and 400B) have slightly higher rate capabilities than those of the samples heat-treated at 700 °C. In contrast, the effect of the type of coating solution (clear solution or colloid-type solution) on capacity was negligible at all C rates, as shown in Figs. 5 and 6. The ionic and electronic conductivities of Li–La–Ti–O layer are dependent on the composition, structure, and phase [20–25]. Moreover, they are affected by the cathode material coming into contact with the Li–La–Ti–O electrolyte [27]. The phase of the coated layer was confirmed as being crystalline with perovskite structure (700A and 700B) or amorphous phase (400A and 400B). Considering the pristine powder and coating material to be the same, it is likely that the better rate capability of 400A and 400B compared with that of 700A and 700B is highly due to the phase of the coating layer. The amorphous phase can offer vacant space for the diffusion of lithium ions and promote lithium ion transfer through the interfaces between the electrode and electrolyte. Another possibility is that different heating temperatures lead to different surface reactions between coating particles and elements on the surface of the pristine powder. A higher temperature facilitates a reaction between coating materials (Li–La–Ti–O) and elements of the pristine powder such as Li, Co, Ni, and Mn, and thus the compositions of the coating layers of 700A and 700B change more than that of 400A and 400B do. Thus, the electrochemical property of a coated sample could be associated with the final composition of the coating layer after heat-treatment.

The cyclic properties of pristine and coated electrode were measured in the voltage range of 4.8–3.0 V at the 1 C rate. Both pristine and coated $Li[Ni_{0.3}Co_{0.4}Mn_{0.3}]O_2$ had stable cyclic performance in the voltage range of 4.6–3.0 V, as presented in Fig. 5. However, when the cut-off charge voltage was 4.8 V, significant capacity fading was observed during cycling. It is known that chemical or structural instability begins in the high voltage range above 4.6 V for the Li[Ni, Co, Mn]O_2 cathode, because of oxygen loss from the lattice in a highly charged state [28]. To examine the effect of the Li–La–Ti–O coating on the cycling behavior under a chemically and structurally unstable condition, the cut-off charge voltage was increased to 4.8 V in this work. As shown in Fig. 7, the coated samples had improved cyclic performance in the voltage range of 4.8–2.0 V, which indicates that the Li–La–Ti–O coating is effective in increasing the chemical and structural stability of $Li[Ni_{0.3}Co_{0.4}Mn_{0.3}]O_2$ in a highly charged state (above 4.6 V). Table 2 summarizes the discharge capacity and capacity retention in the voltage range of 4.8–3.0 V. For a pristine electrode, the capacity retention during 50 cycles was 68.6%. In contrast, the capacity retention increased to 72.5, 71.2, 69.1, and 74.3% for samples 700A, 700B, 400A, and 400B, respectively. Although the Li–La–Ti–O coating did not perfectly suppress the instability, the rapid loss of discharge capacity in the high cut-off voltage range was enhanced by the coating treatment. 400B had better capacity retention than the other samples had.

Thermal stability of the $Li[Ni_{0.3}Co_{0.4}Mn_{0.3}]O_2$ electrode before and after Li–La–Ti–O coating was investigated using DSC analysis in the following test. The electrodes were charged to 4.6 V before the test and sealed in a high-pressure DSC pan. Fig. 8 presents the DSC profiles of pristine and coated $Li[Ni_{0.3}Co_{0.4}Mn_{0.3}]O_2$ electrodes. For the pristine sample, thermal reaction with the electrolyte commenced at roughly ~170 °C and heat was generated until ~270 °C. There were three exothermic peaks including a large peak at ~262 °C. The DSC profile of the coated sample had a slightly different shape. The exothermic peaks of 700A and 700B were clearly distinguished as two small peaks, located at 180–250 °C, and a large peak, located at 180–310 °C. Even though the large peaks of 700A and 700B were sharper than that of the pristine sample, the onset

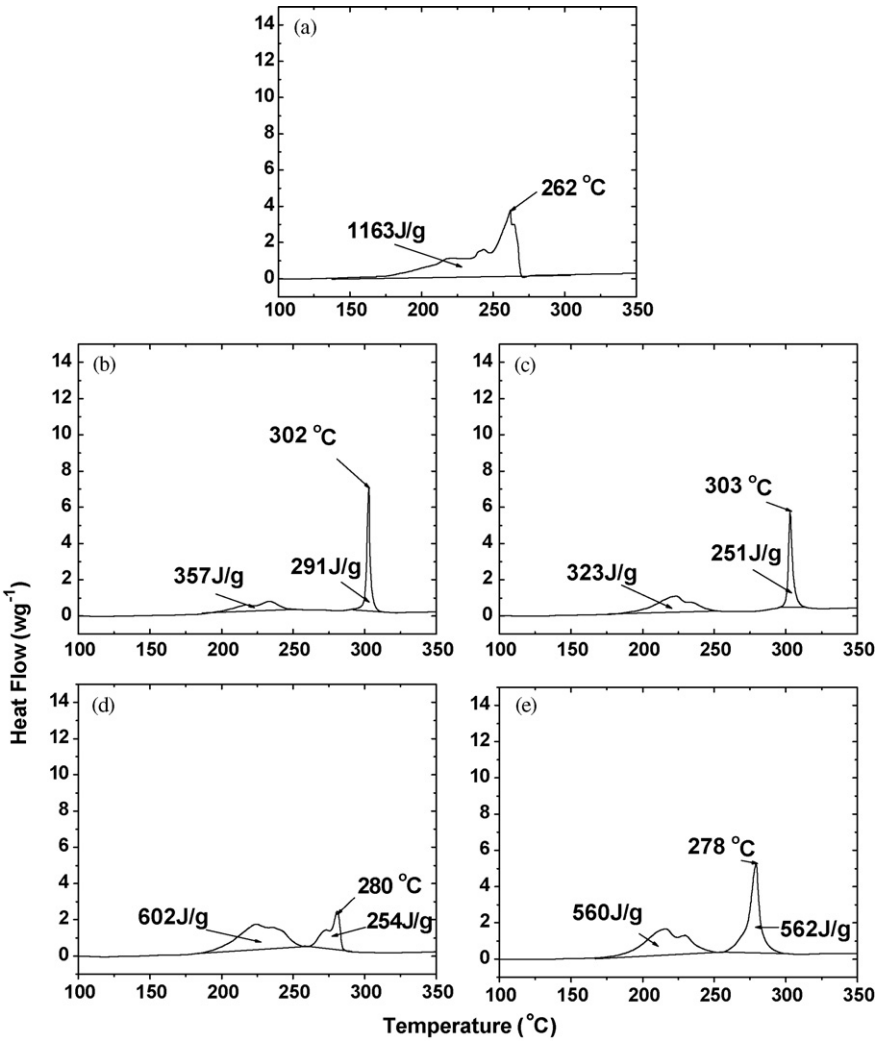

Fig. 8. DSC scans of pristine and surface modified $Li[Ni_{0.3}Co_{0.4}Mn_{0.3}]O_2$ electrodes in a fully charged state (cut-off voltage of 4.6 V). (a) Pristine sample; (b) 700A; (c) 700B; (d) 400A; (e) 400B.

temperature was higher and the heat generation was less, which indicated that the thermal stability was enhanced by the coating treatment. The three exothermic peaks of 400A and 400B were also well separated. The large exothermic peaks of 400A and 400B shifted to a higher temperature of ~280 °C compared with that of the pristine sample. In particular, heat generation for the 400A sample was significantly decreased. Although there was little difference in coating conditions, the exothermic peaks were clearly at higher temperature and heat generation was decreased as well, which indicates that the thermal stability of the $Li[Ni_{0.3}Co_{0.4}Mn_{0.3}]O_2$ electrode was improved by Li–La–Ti–O surface coating, owing to the successful suppression of the surface reaction between electrode and electrolyte by the stable coating.

4. Conclusions

Li–La–Ti–O was introduced as a coating material to improve the electrochemical properties of a $Li[Ni_{0.3}Co_{0.4}Mn_{0.3}]O_2$ cathode. The hydrothermal method was used to obtain uniformly coated samples. The formation of a compact coating layer on the surface of pristine particles was observed by SEM and TEM. XRD and TEM analyses confirmed that the coating layer of the samples heat-treated at 700 °C was a crystalline phase with perovskite structure, but the coating layer of the samples heat-treated at 400 °C was an amorphous phase. The $Li[Ni_{0.3}Co_{0.4}Mn_{0.3}]O_2$ electrode coated with Li–La–Ti–O had an enhanced rate capability compared with the pristine electrode. There is a change in the rate capability according to heat-treatment temperature. The coated samples heat-treated at 400 °C had higher rate capability than those heat-treated at 700 °C. It is expected that the phase (amorphous or crystalline) of the Li–La–Ti–O coating layer may affect the electrochemical characteristics of the coated sample. The cyclic performance of the $Li[Ni_{0.3}Co_{0.4}Mn_{0.3}]O_2$ electrode was improved by Li–La–Ti–O coating under the condition of a high cut-off voltage (4.8 V). DSC showed that the Li–La–Ti–O coating also enhanced the thermal stability of the $Li[Ni_{0.3}Co_{0.4}Mn_{0.3}]O_2$ electrode. Such enhancements are due to the presence of the stable Li–La–Ti–O coating layer, which effectively suppresses reactions between electrode and electrolyte on the surface of the electrode.

Acknowledgement

This work was supported by the Korea Research Foundation Grant funded by the Korean Government (KRF-2008-313-D00451).

References

[1] S. Huang, Z. Wen, X. Yang, Z. Gu, X. Xu, J. Power Sources 148 (2005) 72.
[2] S. Zhang, X. Qiu, Z. He, D. Weng, W. Zhu, J. Power Sources 153 (2006) 350.
[3] K. Amine, J. Liu, I. Belharouak, S.-H. Kang, I. Bloom, D. Vissers, G. Henriksen, J. Power Sources 146 (2005) 111.

[4] Y.J. Park, J.W. Lee, Y.-G. Lee, K.M. Kim, M.G. Kang, Y. Lee, Bull. Korean Chem. Soc. 28 (2007) 2226.
[5] S.-T. Myung, K. Izumi, S. Komaba, Y.-K. Sun, H. Yashiro, N. Kumagai, Chem. Mater. 17 (2005) 3695.
[6] J. Cho, Y.J. Kim, T.-J. Kim, B. Park, Angew. Chem. Int. Ed. Engl. 40 (2001) 3367.
[7] J. Cho, Y.J. Kim, B. Park, Chem. Mater. 12 (2000) 3788.
[8] J. Cho, Y.J. Kim, B. Park, J. Electrochem. Soc. 148 (2001) A1110.
[9] K. Amine, H. Yasuda, M. Yamachi, Electrochem. Solid-State Lett. 3 (2000) 178.
[10] M.M. Thackeray, C.S. Johnson, J.-S. Kim, K.C. Lauzze, J.T. Vaughey, N. Dietz, D. Abraham, S.A. Hackney, W. Zeltner, M.A. Anderson, Electrochem. Commun. 5 (2003) 752.
[11] S.-T. Myung, K. Izumi, S. Komaba, H. Yashiro, H.J. Bang, Y.K. Sun, N. Kumagai, J. Phys. Chem. C 111 (2007) 4061.
[12] H. Lee, Y. Kim, Y.S. Hong, Y. Kim, M.G. Kim, N.-S. Shin, J. Cho, J. Electrochem. Soc. 153 (2006) A781.
[13] J. Cho, H. Kim, B. Park, J. Electrochem. Soc. 151 (2004) A1707.
[14] K.S. Ryu, S.H. Lee, B.K. Koo, J.W. Lee, K.M. Kim, Y.J. Park, J. Appl. Electrochem. 38 (2008) 1385.
[15] J. Cho, Y.W. Kim, B. Kim, J.G. Lee, B. Park, Angew. Chem. Int. Ed. 42 (2003) 1618.
[16] Y. Wu, A.V. Murugan, A. Manthiram, J. Electrochem. Soc. 155 (2008) A635.
[17] G.R. Hu, X.R. Dengm, Z.D. Peng, Ke. Du, Electrochim. Acta 53 (2008) 2567.
[18] J.M. Zheng, Z.R. Zhang, X.B. Wu, Z.X. Dong, Z. Zhu, Y. Yang, J. Electrochem. Soc. 155 (2008) A775.
[19] B.-C. Park, H.-B. Kim, S.-T. Myung, K. Amine, I. Belharouak, S.-M. Lee, Y.-K. Sun, J. Power Sources 178 (2008) 826.
[20] K.Y. Yang, K.Z. Fung, I.C. Leu, J. Alloys Compd. 438 (2007) 207.
[21] J.M. Lee, S.H. Kim, Y.S. Tak, Y.S. Yoon, J. Power Sources 163 (2006) 173.
[22] Y. Inaguma, L. Chen, M. Itoh, T. Nakamura, T. Uchida, H. Ikuta, M. Wakihara, Solid State Commun. 86 (1993) 689.
[23] Y. Inaguma, L. Chen, M. Itoh, T. Nakamura, Solid State Ionics 70–71 (1994) 196.
[24] Y. Inaguma, J. Yu, Y.J. Shan, M. Itoh, T. Nakamura, J. Electrochem. Soc. 142 (1995) L8.
[25] M. Oguni, Y. Inaguma, M. Itoh, T. Nakamura, Solid State Commun. 91 (1994) 627.
[26] H. Zhao, L. Gao, W. Qiu, X. Zhang, J. Power Sources 132 (2004) 195.
[27] C.L. Liao, C.H. Wen, K.Z. Fung, J. Alloys Compd. 432 (2007) L22.
[28] J. Choi, A. Manthiram, J. Electrochem. Soc. 152 (2005) A1714.